Study on Structural and Thermoelectric Properties of $Fe_{2+x}Ni_{1-x}Ti$ (x=0, 0.25, 0.5) based Intermetallics: A First-Principles DFT Study

Shabeer Ali PC[1,3,a], Manoj Raama Varma[2,3,b], KN Narayanan Unni[1,3,c]

[1] *Centre for Sustainable Energy Technologies, CSIR-National Institute for Interdisciplinary Science and Technology (CSIR-NIIST), Industrial Estate, P.O. Thiruvananthapuram-695019, India.*

[2] *Materials Science and Technology Division, CSIR- National Institute for Interdisciplinary Science and Technology (CSIR-NIIST), Industrial Estate, P.O., Thiruvananthapuram-695019, India.*

[3] *Academy of Scientific and Innovative Research (AcSIR), Ghaziabad-201002, India.*

[a] shabeeralionline7@gmail.com

[b] manoj@niist.res.in

[c] unni@niist.res.in

Abstract

The structural, electronic, and thermoelectric properties of the series of full heusler alloys Fe_2NiTi and its $Fe_{2+x}Ni_{1-x}Ti$ (x=0, 0.25, 0.5) have been investigated theoretically. Here, we primarily concentrate on the thermoelectric properties of this new class of Heusler compounds, known as all-3d Heusler alloys. A_2BTi type alloys of Fe_2NiTi and its Fe (Iron) excess in Ni (Nickel) sites like $Fe_{2+x}Ni_{1-x}Ti$ (x=0, 0.25, 0.5) were studied using Density Functional Theory (DFT) and predicted the electronic structure and thermoelectric properties. The WIEN2k code's implementation of the full potential linearized augmented plane wave (FP-LAPW) method is a framework for first-principle computations. The electronic structure shows the material is metallic. The Seebeck coefficient (S) is found to increase, and the thermoelectric power factor is found to decrease with Fe addition on the Ni sites due to the increase in thermal (κ) and decrease in electrical conductivity (σ).

Keywords: Density Functional Theory, FP-LAPW, GGA-PBE, WIEN2k code, BoltzTraP code.
Received 29 January 2025; First Review 19 March 2025; Accepted 30 March 2025.

*** Address of correspondence**
Shabeer Ali PC
Centre for Sustainable Energy Technologies, CSIR-National Institute for Interdisciplinary Science and Technology (CSIR-NIIST), Industrial Estate, P.O. Thiruvananthapuram, 695019, India.

Email: shabeeralionline7@gmail.com

How to cite this article
Shabeer Ali PC, Manoj Raama Varma, KN Narayanan Unni, Study on Structural and Thermoelectric Properties of $Fe_{2+x}Ni_{1-x}Ti$ (x=0, 0.25, 0.5) based Intermetallics: A first-principles DFT Study, J. Cond. Matt. 2025; 03 (02): 77-82.

Available from:
https://doi.org/10.61343/jcm.v3i02.98

Introduction

Thermoelectric (TE) materials have garnered considerable interest in the quest for efficient energy conversion and advanced technological applications. With their unique properties and potential applications, these materials offer innovative solutions to some of the most pressing challenges in energy and technology[1-3]. Thermoelectric materials are pivotal in advancing energy conversion technologies, particularly waste heat recovery and power generation. These materials, which can directly convert temperature differentials into electric voltage and vice versa, have gained considerable attention due to their potential to create sustainable energy solutions [4].

Computational techniques have been essential to discover novel TE materials with economically viable performance in recent years. DFT has become one of these techniques that is particularly effective in predicting the characteristics of materials [5]. We used DFT to study the thermoelectric and magnetic properties in the present investigation.

The thermoelectric characteristics of this new class of A_2BC Heusler compound, referred to as an all-3d Heusler alloy, are quite promising [6, 7]. Fe_2NiTi crystallizing in the $C1_b$ structure has been taken as the parent material. This alloy possesses quite tunable characteristics by changes in the phase compositions, doping, and site disorder. Heusler alloys have a significant magneto crystalline anisotropy, as shown in several investigations [8]. The anisotropy may also be tuned by interstitial doping, strain, and local atom ordering, making them a promising contender for permanent magnet applications. Here, we primarily concentrate on the thermoelectric characteristics of this new class of Heusler compounds [9].

Fe_2NiTi has a high electrical resistivity (120 μΩcm), a medium compressive strain (5%), and a high compressive

strength (1280 MPa) [10]. In the current study, we used first-principles calculations using the full potential linearized augmented plane wave (FP-LAPW) approach, which is employed in the WIEN2k program, to determine the structural and electrical characteristics of $Fe_{2+x}Ni_{1-x}Ti$ (x=0,0.25,0.5) [11-13]. The thermoelectric properties of the same system have also been examined using the semi-classical Boltzmann transport theory. The Perdew–Burke–Ernzerhof (PBE) framework includes the Generalized Gradient Approximation (GGA) to handle the exchange-correlation effects [14]. Hence, in the present investigation, we report our theoretically predicted thermoelectric characteristics, such as the power factor, figure of merit, thermal conductivity, electrical conductivity, and Seebeck coefficient.

Method

The density functional theory implemented through the WIEN2K program is used for theoretical calculations [15]. The full-potential linearized enhanced plane-wave method (FPLAPW) is the cornerstone of this package. According to our calculations, RMT is the minimum radius, and Kmax is the highest reciprocal lattice vector; $RMT \times K_{max}$ is set at 7, and RMT is the unit cell's smallest atomic sphere radii, while K_{max} is the plane wave cut-off. We selected the Perdew-Burke Ernzerhof generalized gradient schemes (PBE-GGA) as the exchange-correlation potential in our calculation. For Fe and Ni atoms, the muffin-tin radii were set at 2.3 atomic units, while for Ti atoms, they were set at 2.24. The maximum value for partial waves within the muffin-tin spheres was expanded in spherical harmonics up to l_{max}=10 to accomplish energy and charge convergence. An energy cutoff of −6.0 Ryd and 5000 k points were used for these calculations., The stable structure was produced, assuming the self-consistency converged at a total energy of 0.00001 Ry. The exchange-correlation potential considered in the calculations GGA-PBE is given as

$$E_{xc}^{GGA-PBE} = \int \epsilon_{xc}^{PBE}(\rho, \nabla\rho)\, d^3r \qquad (1)$$

E_{xc} denotes the exchange-correlation energy and ϵ_{xc}^{PBE} represents the PBE exchange-correlation energy density as a function of the electron density ρ and its gradient $\nabla\rho$ [16].

The Kohn–Sham (K-S) equations are a set of one-electron equations derived from DFT. These maps the many-body problem of interacting electrons and nuclei and are the primary framework for first principles computations. The linearized-augmented-plane-wave (LAPW) approach, which is used, for instance, in the computer code WIEN2k to explore crystal characteristics on the atomic scale, is one of the most accurate ways to solve the K-S equations [17]. APW + local orbital method (linearized) is a sophisticated computer method used to calculate the electronic structure of solids using DFT. The self-consistent field (SCF)technique aims to achieve self-consistency between the input and output electron densities or potentials.

By minimizing the total energy functional for the electron density, the DFT variational technique ensures that the estimated ground state energy is an upper bound on the actual ground state energy [18, 19]. The system's absolute ground state density and ground state energy are determined by repeatedly solving the Kohn-Sham equations using the SCF technique. With reasonable computational effort, this method enables DFT to characterize the electronic structure of many-electron systems precisely [20, 21].

The total energy minimization method using Birch-Murnaghan's equation of state has been used to optimize the equilibrium lattice parameters of $Fe_{2+x}Ni_{1-x}Ti$ (x=0, 0.25, 0.5). The energy curve's minimal value shows the equilibrium condition of the system. The ground-state energy with the associated ground-state volume has the lowest energy. The lattice parameters were computed using the minimal volume.

The package BoltzTraP, which contains the Boltzmann transport characteristics program for computing semi-classical transport coefficients, was used for thermoelectric calculations. This software, which relies on the density functional theory within the FPLAPW technique, is interfaced with the WIEN2k code.

Discussion

1. Structural Properties

Fig 1-(a,b) are the generated crystal structures of the samples using the software XCrysDen with a new molecular surface with constant Gaussian function having pseudo-density surface type of resolution about 0.035 Å. Theoretically calculated structures of the first sample Fe_2NiTi is optimized successfully with space group F-43m (No. #216) having Cubic symmetry with a lattice parameter of 5.83 Å. This value is very close to the experimental value of the structural lattice parameter reported by Marathe et al. [22] and YANG Jihan et al [23]. For the second sample, $Fe_{2.25}Ni_{0.75}Ti$, the volume is optimized with a space group of P-43m (No. #215) with a lattice parameter of 5.827 Å,

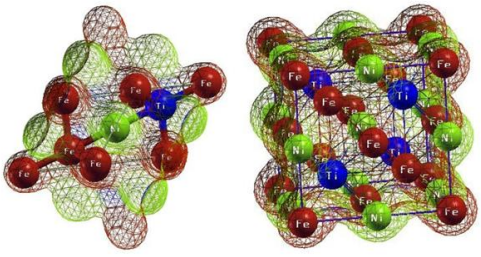

Figure 1: *Type A_2BC unit cells for common Heusler alloys: (a) primitive 4-atom unit cell (b) conventional 16-atom unit cell.*

Table 1: The calculated lattice constants (a_0, c_0) in (Å), bulk modulus (B) in (G_{pa}), volume in ($Å^3$), the derivative of bulk modulus (B'), and the ground state energy (eV) for $Fe_{2+x}Ni_{1-x}Ti$ (x=0, 0.25, 0.5).

Compound	a_0 (Å)	c_0 (Å)	V ($Å^3$)	B (G_{Pa})	B'	E_o (eV)
Fe_2NiTi	5.8268	—	333.77	162.98	12.95	-9840.53
$Fe_{2.25}Ni_{0.75}Ti$	5.8270	—	1335.14	114.82	0.12	-38866.09
$Fe_{2.5}Ni_{0.5}Ti$	4.1123	5.8140	663.5318	178.84	5.14	-19185.02

and the third sample, $Fe_{2.5}Ni_{0.5}Ti$ has tetragonal symmetry with space group of P-4m2 (No. #115) with lattice parameter of a=4.1123 Å and c/a=1.41. The stable phase of these structures has been determined by analysing the structural characteristics using Birch–Murnaghan's equation of state, which describes the energy of a solid as a function of volume given below

$$E(V) = E_o + \frac{9V_oB_o}{16}\left\{\left[\left(\frac{V_o}{V}\right)^{\frac{2}{3}} - 1\right]^3 B_o' + \left[\left(\frac{V_o}{V}\right)^{\frac{2}{3}} - 1\right]^2 \left[6 - 4\left(\frac{V_o}{V}\right)^{\frac{2}{3}}\right]\right\} \quad -(2)$$

Fitting the total energy versus volume of the unit cell is being done as shown in Fig. 2(a-c) [24]. In this equation of state, E_0, B_0, V_0, V, and B are the minimum energy, bulk modulus, reference volume, deformed volume, and derivative of the bulk modulus with respect to pressure, respectively, shown in Table 1.

2. Electronic Properties

The energy band gap and density of states Fig. 3 (a-f) show the band structures of Fe_2NiTi, $Fe_{2.25}Ni_{0.75}Ti$, and $Fe_{2.5}Ni_{0.5}Ti$ samples along the first Brillouin zone's $W - L - \Lambda - \Gamma - \Delta$ -X$- Z - W - K$ high symmetry directions. Our band structure plots show that all the materials are metallic.

The conduction band minimum and valence band maximum indicate the boundaries for the electronic band gap and the zero-energy reference in eV is Fermi level E_F. It reveals that the compositions are metallic as the conduction and valance bands overlap. The total density of states (TDOS) and partial density of states (PDOS) provide further insight into the electronic properties and the contribution of individual atoms toward the band structure. We can see that in Fig.4(a-f) that Fe, Ni, and Ti atom's s and p states of Fe_2NiTi, $Fe_{2.25}Ni_{0.75}Ti$, and $Fe_{2.5}Ni_{0.5}Ti$ has very small contributions to the band structure. In addition, their d state significantly contributes to the conduction band compared to its s and p states. The transition metal atom's d states are found to be crossing the Fermi level in these compositions, giving rise to their metallic nature.

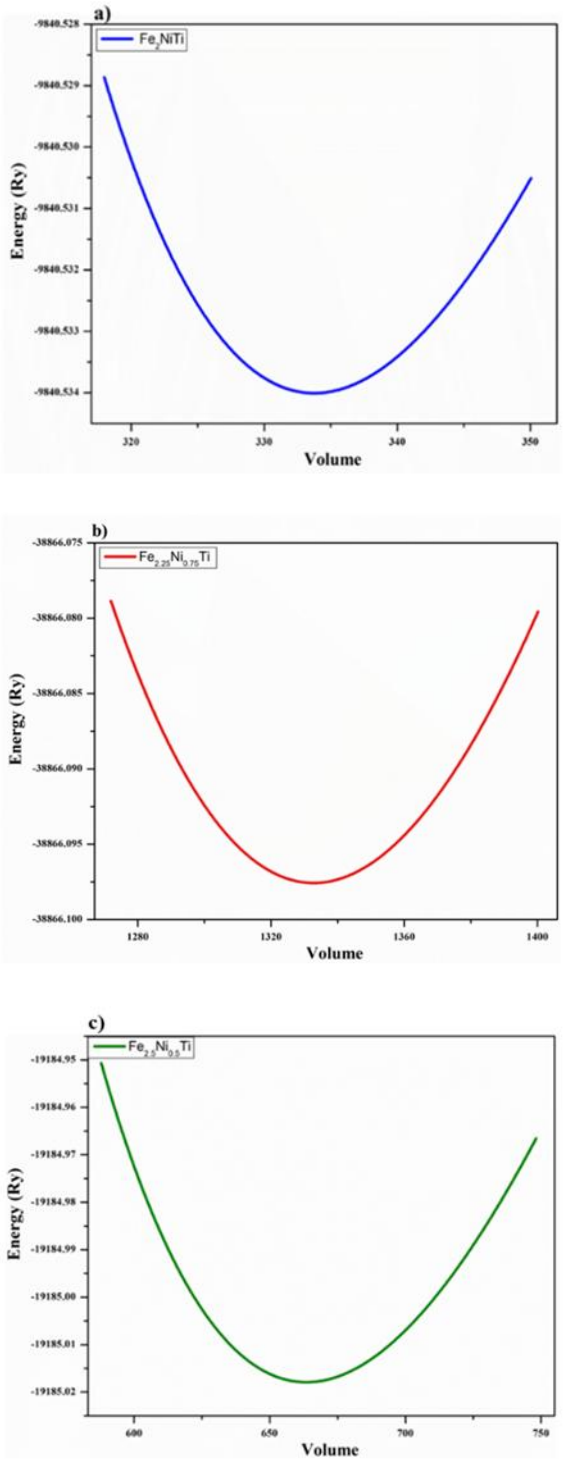

Figure 2: Energy versus volume curves of the optimized structure of **a)** Fe_2NiTi, **b)** $Fe_{2.25}Ni_{0.75}Ti$, and **c)** $Fe_{2.5}Ni_{0.5}Ti$ alloys.

3. Thermoelectric Properties

We used semi-classical Boltzmann transport theories based on a smoothed Fourier interpolation of the bands, as implemented in the BoltzTraP code, to investigate the thermoelectric characteristics of the compounds [11]. Fig.5(indicates calculated thermoelectric parameters as a

function of temperature at the Fermi level, including the Seebeck coefficient, electrical conductivity, electronic thermal conductivity (κ_e), and power factor ($S^2\sigma$). l. Fig.5-a, b displays the Seebeck coefficient for the compositions $Fe_{2+x}Ni_{1-x}Ti$ (x = 0, 0.25, 0.5). In Fe_2NiTi, both spin

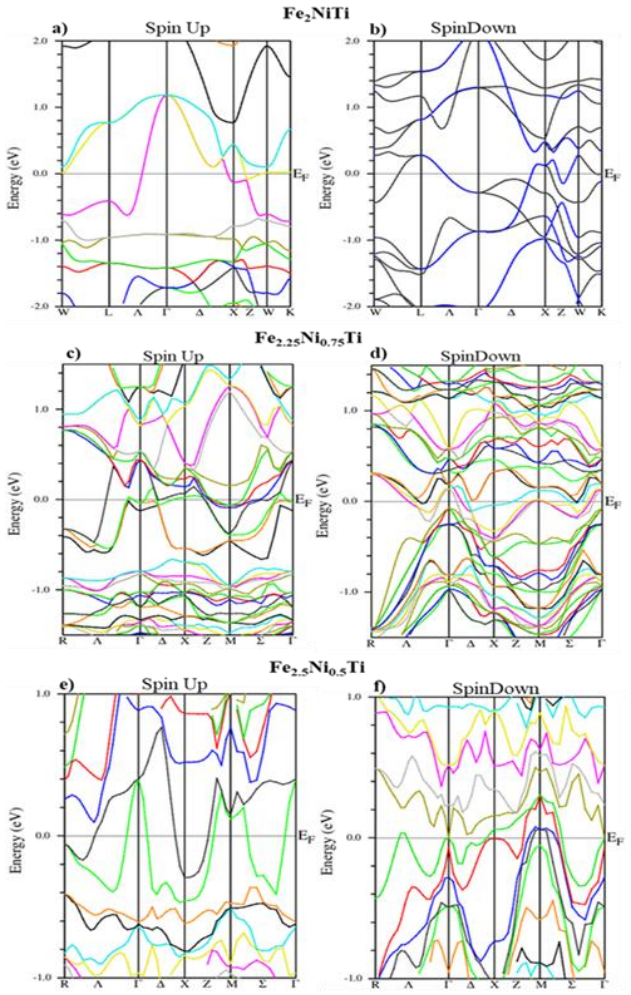

Figure 3: Spin up and spin down energy Band structures of Fe_2NiTi, $Fe_{2.25}Ni_{0.75}Ti$, and $Fe_{2.5}Ni_{0.75}Ti$.

channels have negative Seebeck values, indicating that it is an n-type material. It shows a Seebeck value of -1.5 µV/K at the spin-up channel and -35 µV/K at the spin-down channel at room temperature. $Fe_{2.5}Ni_{0.5}Ti$ is found to be a p-type material. In the case of $Fe_{2.25}Ni_{0.75}Ti$, both spin-up and spin-down channels show a negative Seebeck coefficient, indicating that it is an n-type material. S values attain their room temperature value of -15 µV/K value, which remains a constant throughout the temperature range of 100 to 900 K. From the plots, it can be noticed that the maximum value of the Seebeck coefficient is S~ 11.5 µV/K for $Fe_{2.5}Ni_{0.5}Ti$ spin up channel and 7.5 µV/K at room temperature, and it goes on decreasing with increasing temperature. $Fe_{2.5}Ni_{0.5}Ti$ also has a positive Seebeck value of 2.5 µV/K with an increasing Seebeck coefficient increasing with temperature, and this compound has both spin channels showing positive values for the Seebeck coefficient.

The total Seebeck coefficient value of the samples, using the spin up and spin down channel values, are calculated using $S_{tot}=(S\uparrow\sigma\uparrow+S\downarrow\sigma\downarrow)/\sigma_{tot}$ where $\sigma_{tot}=\sigma\uparrow+\sigma\downarrow$ [5], is shown in Fig 5-b. It is visible that $Fe_{2.5}Ni_{0.5}Ti$ has a positive value of Seebeck with 5.5 µV/K at room temperature and the other [14] two samples have negative values, -16 µV/K and –

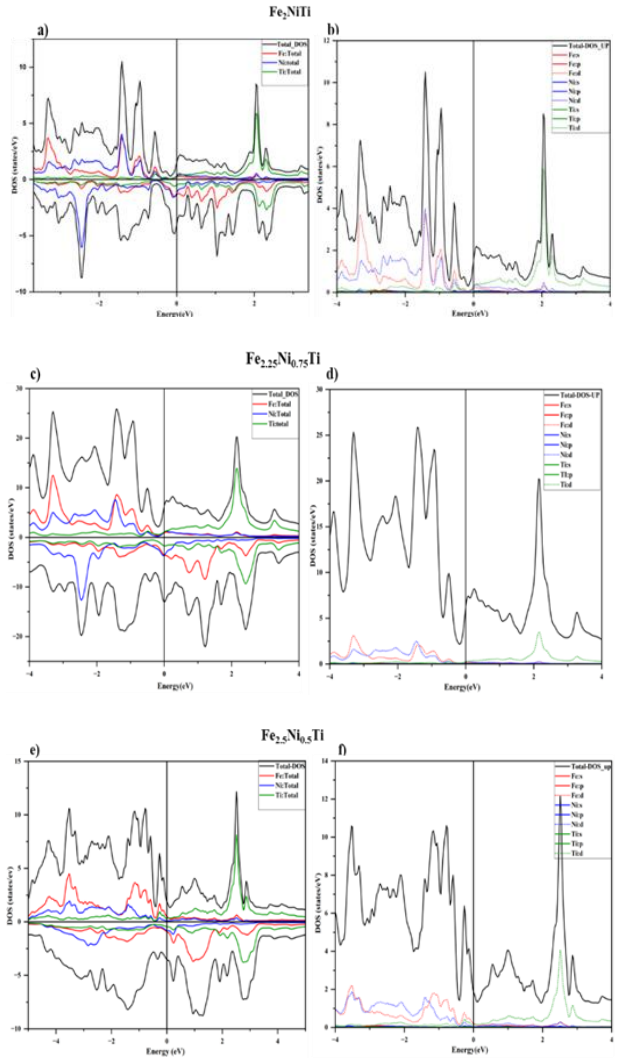

Figure 4 (a-f). Total DOS/PDOS OF (a-b) Fe_2NiTi, (c-d) $Fe_{2.25}Ni_{0.75}Ti$, and (e-f) $Fe_{2.5}Ni_{0.5}Ti$.

20 µV/K for $Fe_{2.25}Ni_{0.5}Ti$ and Fe_2NiTi respectively [5]. The Seebeck plot shows the different trends in the sample's different spin channels; at room temperature, the Seebeck coefficient reaches its highest value; at higher temperatures, it reaches its minimal value. The decreasing trend in the Seebeck coefficient may be related to increased charge carrier concentration with increasing temperatures.

Better and more efficient thermoelectric material needs high values of electrical conductivity. The highest electrical conductivity per relaxation time exhibited at room temperature is $3.6\times10^{20}\ \Omega^{-1}m^{-1}s^{-1}$ of Fe_2NiTi, and the lowest value of $1.5\times10^{20}\ \Omega^{-1}m^{-1}s^{-1}$ for $Fe_{2.25}Ni_{0.5}Ti$. Low thermal conductivity values are needed for a better figure of merit. $Fe_{2.25}Ni_{0.75}Ti$ spin down has the smallest value with 1

W/(mKs) and the highest value of 2.5 W/(mKs) for Fe_2NiTi spin down channel, and all materials show increased thermal conductivity with temperature. The power factor (PF), given by $S^2\sigma$, indicates how well a material converts heat into electricity. Fe_2NiTi spin-up has a good power factor value of 45×10^{10} $Wm^{-1}K^{-2}s^{-1}$; the remaining samples have very low ranges compared to this. Fig 5-d shows total spins power factor values, making it clear that Fe_2NiTi has the highest value of 26×10^{10} $Wm^{-1}K^{-2}s^{-1}$ and $Fe_{2.25}Ni_{0.75}Ti$ and $Fe_{2.5}Ni_{0.5}Ti$ have PF values viz. 9.5×10^{10} $Wm^{-1}K^{-2}s^{-1}$ and 1.5×10^{10} $Wm^{-1}K^{-2}s^{-1}$ respectively. As temperature increases, the power factor also increases. This is because metals have a dominant electronic contribution to thermal conductivity, where the movement of free electrons primarily carries heat energy. generally, this contribution has a direct correlation with electrical conductivity. According to the Wiedemann-Franz law, the electronic component of thermal conductivity rises with temperature, raising the overall power factor. Because of their excellent thermoelectric response, these compositions offer a good energy-harvesting option for thermoelectric devices.

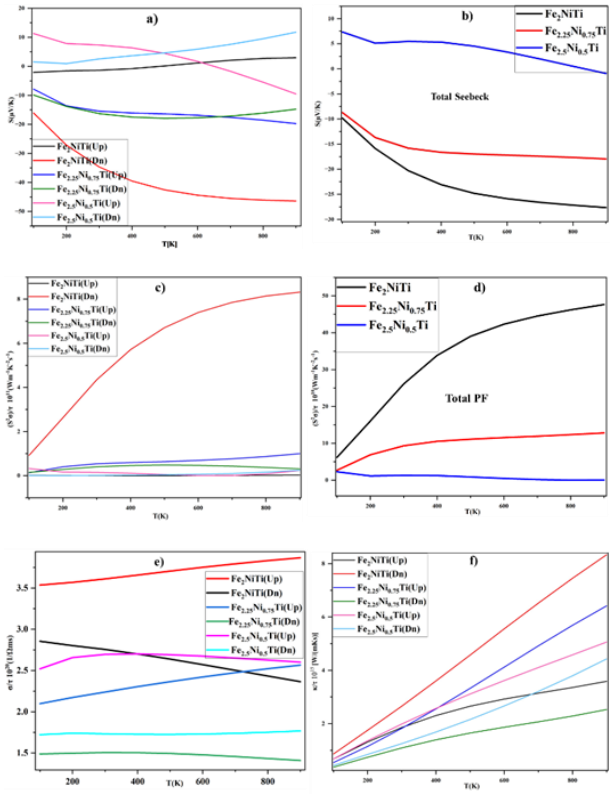

Figure 5: a) Seebeck effect for both spins, **b)** Total Seebeck effect of three samples, **c)** Electrical conductivity **d)** Power factor for both the spin channels, **e)** Total power factor value of three samples, **f)** Thermal conductivity.

The figure of merit (ZT) as a function of temperature from 100 K to 900 K is shown in Fig. 6. Fe_2NiTi has the highest ZT value at 900 K. The ZT values for the Fe_2NiTi, $Fe_{2.25}Ni_{0.75}Ti$, and $Fe_{2.5}Ni_{0.5}Ti$ alloys are 0.045, 0.012, and 0.0046, respectively.

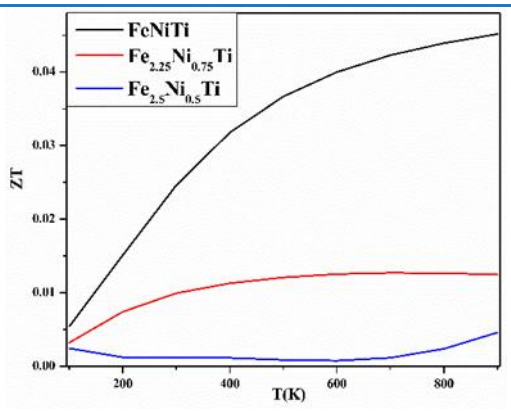

Figure 6: Figure of merit of Fe_2NiTi, $Fe_{2.25}Ni_{0.75}Ti$, and $Fe_{2.5}Ni_{0.5}Ti$.

Conclusion and Future Prospective

DFT-based WIEN2k code examines the structural, electronic, and thermoelectric properties of the Fe-based $Fe_{2+x}Ni_{1-x}Ti$ (x=0, 0.25, 0.5). It has been found that the stable, optimized structure of Fe_2NiTi and $Fe_{2.25}Ni_{0.75}Ti$ have space group of cubic with F-43m (No. #216) and P-43m (No. #215), respectively, while $Fe_{2.5}Ni_{0.5}Ti$ has a tetragonal structure with space group of P-4m2 (No. #115). Calculated structural parameters agree with the reported experimental values. The full potential linearized augmented-plane-wave method within the WIEN2k code was used for the calculations. The metallic nature of these materials stems from their electronic structure derived using band structure and DOS calculations using DFT with spin-orbit coupling. Thermoelectric properties show positive Seebeck for $Fe_{2.5}Ni_{0.5}Ti$ and negative value of Seebeck for Fe_2NiTi, $Fe_{2.25}Ni_{0.75}Ti$.

Acknowledgment

SA, MRV, and KNU thank the director of the CSIR-NIIST institution for the laboratory facilities. SA would like to acknowledge the financial assistance from CSIR-SRF (File. No.: 31/038(0604)/2019-EMR-I, India is duly acknowledged with gratitude. MRV would like to thank CSIR-HRDG for the kind support as an Emeritus Scientist Project.

References

1. S. Yang, P.Q., L. Chen and X. Shi, *Recent Developments in Flexible Thermoelectric Devices*, Small Sci., 2021, 1, 2100005.
2. Mardi, S., et al., *The interfacial effect on the open circuit voltage of ionic thermoelectric devices with conducting polymer electrodes.* Advanced Electronic Materials, 2021. **7**(12): p. 2100506.
3. Zhang, C., et al., *Gibbs Adsorption and Zener Pinning Enable Mechanically Robust High-Performance Bi_2Te_3-Based Thermoelectric Devices.* Advanced Science, 2023. **10**(26): p. 2302688.

4. Hou, Y., et al., *Programmable and Surface-Conformable Origami Design for Thermoelectric Devices.* Advanced Science, 2024. **11**(10): p. 2309052.
5. Gutiérrez Moreno, J.J., et al., *A review of recent progress in thermoelectric materials through computational methods.* Materials for Renewable and Sustainable Energy, 2020. **9**(3): p. 16.
6. Marathe, M. and H.C. Herper, *Exploration of all-3 d Heusler alloys for permanent magnets: An ab initio based high-throughput study*. Physical Review B, 2023. 107(17): p. 174402.
7. Tas, M., et al., *High Spin Magnetic Moments in All-3 d-Metallic Co-Based Full Heusler Compounds.* Materials, 2023. **16**(24): p. 7543.
8. Matsushita, Y., et al., *Large magnetocrystalline anisotropy in tetragonally distorted Heuslers: a systematic study.* Journal of Physics D: Applied Physics, 2017. **50**(9): p. 095002.
9. Herper, H.C., *Ni-based Heusler compounds: How to tune the magnetocrystalline anisotropy*. Physical Review B, 2018. **98**(1): p. 014411.
10. YAN, H.-L., et al., *Phase Stability, Magnetism and Mechanical Properties of A2BTi: Ab-initio Calculations and Experimental Studies.* Acta Metall Sin, 2023: p. 0-0.
11. Singh, D.J. and L. Nordstrom, *Planewaves, Pseudopotentials, and the LAPW method*. 2006: Springer Science & Business Media.
12. Grad, G.B. and E.V. Bonzi, *First principles study of the binding energies of pure metals using FP-LAPW method.* Journal of Electron Spectroscopy and Related Phenomena, 2013. **189**: p. 45-50.
13. Benkraouda, M. and N. Amrane, *Full potential linear augmented plane wave calculations of Electronic and Optical properties in ZnO.* Journal: JOURNAL OF ADVANCES IN PHYSICS. **11**(5).
14. Yan, J., et al., *Material descriptors for predicting thermoelectric performance.* Energy & Environmental Science, 2015. **8**(3): p. 983-994.
15. Wang, S., et al., *Assessing the Thermoelectric Properties of Sintered Compounds<? format?> via High-Throughput Ab-Initio Calculations.* Physical Review X, 2011. **1**(2): p. 021012.
16. Kohn, W., *Nobel Lecture: Electronic structure of matter—wave functions and density functionals.* Reviews of Modern Physics, 1999. **71**(5): p. 1253.
17. Koch, W. and M.C. Holthausen, *A chemist's guide to density functional theory*. 2015: John Wiley & Sons.
18. Singh, R. and B.M. Deb, *Developments in excited-state density functional theory.* Physics reports, 1999. **311**(2): p. 47-94.
19. Levi, G., A.V. Ivanov, and H. Jónsson, *Variational calculations of excited states via direct optimization of the orbitals in DFT.* Faraday Discussions, 2020. **224**: p. 448-466.
20. Perdew, J., K. Burke, and M. Ernzerhof, *Phys Rev Lett 77: 3865, Errata:(1997).* Phys. Rev. Lett., 1996. **78**: p. 1396.
21. Kohn, W. and L.J. Sham, *Self-consistent equations including exchange and correlation effects.* Physical review, 1965. **140**(4A): p. A1133.
22. Marathe, M.a.H.C.H., *Exploration of all-3 d Heusler alloys for permanent magnets: An ab initio based high-throughput study*. Physical Review B, 2023. 107(17): p. 174402.
23. YANG Jinhan, Y.H., LIU Haoxuan, ZHAO Ying, YANG Yiqiao, ZHAO Xiang, ZUO Liang. *Phase Stability, Magnetism, and Mechanical Properties of A2BTi: First-Principles Calculations and Experimental Studies*. Acta Metall Sin, 2024, 60(12): 1701-1709.
24. Katsura, T. and Y. Tange, *A simple derivation of the Birch–Murnaghan equations of state (EOSs) and comparison with EOSs derived from other definitions of finite strain*. Minerals, 2019. 9(12): p. 745.